Mathematical Model for Diffusion of a Protein and a Precipitant about a Growing Protein Crystal in Microgravity

ONOFRIO ANNUNZIATA[a,b] AND JOHN G. ALBRIGHT[a]

[a]*Department of Chemistry, Texas Christian University, Fort Worth, Texas, USA*

[b]*Department of Physics, Massachusetts Institute of Technology, Cambridge, Massachusetts, USA*

ABSTRACT: Equations are presented that model diffusion of a protein to the surface of a growing crystal in a convection-free environment. The equations apply to crystal growth solutions that contain both a protein and a protein precipitant. The solutions are assumed ternary and the equations include all four diffusion coefficients necessary for the full description of the diffusion process. The four diffusion coefficients are assumed constant. Effects of crystal/solution moving boundary and the effect of a protein adsorption barrier at the crystal interface are included. The equations were applied to the system lysozyme chloride + NaCl + H_2O, which has served as the primary model system for the study of crystal growth of proteins and for which there are now published ternary diffusion coefficients. Calculated results with and without the inclusion of cross-term diffusion coefficients are compared.

KEYWORDS: multicomponent; diffusion; crystal growth; microgravity; lysozyme; NaCl

INTRODUCTION

Obtaining protein crystals of good structural quality is often the main issue for three dimensional, atomic resolution structure studies of biological macromolecules. Crystallization is an intrinsically non-equilibrium process, and concentration gradients occur around the crystal. The protein crystallizes, reducing its concentration at the moving face of the growing crystal. This creates a protein gradient between the bulk solution and the crystal. This gradient, in turn, causes multicomponent diffusive transport of protein and precipitant. The salt may move toward or away from the crystal face due to the concentration gradient of the protein adjacent to the crystal face and depending on the sign of D_{21}.[1–3] The gradients produced are related to several mechanisms: both the intrinsic kinetic rates of crystal growth and transport to the crystal surface determine the path the system takes toward equilibrium. Any variable, whose change modifies those processes, changes the properties of the resultant final crystal.

Address for correspondence: John G. Albright, Department of Chemistry, Box 298860, Texas Christian University, Fort Worth, TX 76129, USA.
j.Albright@tcu.edu

Ann. N.Y. Acad. Sci. **974: 610–624 (2002).**

Crystallization experiments conducted under microgravity conditions have yielded protein crystals that provide diffraction data of significantly higher resolution than the best crystals of these proteins grown under normal gravity conditions.[3] Since a clear difference between microgravity and normal gravity based experiments is the magnitude of the buoyancy forces in the solution, the role of convection in protein crystal growth is of great interest.

Lin *et al.*[2] have analyzed, by numerically modeling lysozyme crystal growth, the difference between the concentration fields that occur at $0\,g$ and $1\,g$ around a crystal. With convection, the lysozyme concentration in the bulk solution is more uniform. At $0\,g$, a concentration depletion zone of considerable width develops about the growing crystal. Such boundary layers, in which the probability for nucleation of parasitic crystals is strongly reduced, have often been cited as a reason for obtaining better protein crystal in microgravity. Lin *et al.*[2] also raised the issue of coupled transport between protein and precipitant. However, the lack of information on the protein-salt transport interaction has made it difficult to develop accurate and meaningful models.

In this paper, a mathematical model is developed for describing the concentration profiles around a growing spherical crystal in a microgravity environment, in which convection is not considered.

GEOMETRY OF THE MODEL

The geometry of the model is based on a spherical crystal surrounded by an aqueous fluid containing protein and precipitant. This configuration can be prepared experimentally by adding a crystal to a uniform supersaturated solution in a microgravity environment. However, it is important to note that, due to vibrations on the spacecraft, the crystal may move within the solution. We do not consider this effect in the model. The dimensions of the cell are considered large with respect to the size of the crystal contained inside. Model symmetry, together with other reasonable assumptions, furnishes analytic solutions of the concentration profiles around the crystal. In a real experiment, the dimensions of the crystal may not be negligible relative to the size of the cell, and the crystal shape will not be spherical.[4] Nevertheless, the aim of the model is to highlight the role of the coupled diffusion and relate the effects to only a few relevant variables.

Fick's second law is the cardinal equation for the model:

$$\begin{aligned} \frac{\partial c_1}{\partial t} &= D_{11}\nabla^2 c_1 + D_{12}\nabla^2 c_2, \\ \frac{\partial c_2}{\partial t} &= D_{21}\nabla^2 c_1 + D_{22}\nabla^2 c_2. \end{aligned} \tag{1}$$

Subscript "1" denotes the protein and "2" the precipitant, c_i is the molar concentration of species i, D_{ij} denotes a diffusion coefficient (the volume frame reference is assumed), and t is the time. For a spherical crystal, it is convenient to express the Laplacian in spherical coordinates. In this representation, in fact, the radial distance from the center of the crystal r is the only position variable. We can transform the concentration Laplacian into[5]

$$\nabla^2 c_i = \frac{\partial^2 c_i}{\partial r^2} + \frac{2}{r}\frac{\partial c_i}{\partial r}, \tag{2}$$

and by setting $\gamma_i = c_i r$, from **(1)** we obtain

$$\begin{aligned} \frac{\partial \gamma_1}{\partial t} &= D_{11}\frac{\partial^2 \gamma_1}{\partial r^2} + D_{12}\frac{\partial^2 \gamma_2}{\partial r^2}, \\ \frac{\partial \gamma_2}{\partial t} &= D_{21}\frac{\partial^2 \gamma_1}{\partial r^2} + D_{22}\frac{\partial^2 \gamma_2}{\partial r^2}. \end{aligned} \tag{3}$$

INITIAL CONDITIONS

As an initial condition (time $t = 0$), we assume the solution to have uniform concentrations of all components throughout; that is,

$$c_i = c_i^0, \ \gamma_i = c_i^0 r = \gamma_i^0 \quad (i = 1, 2). \tag{4}$$

Several partial differential equations can be reduced to ordinary differential equations by performing the Laplace transformation $L\{\cdot\}$ that incorporates the initial conditions. The Laplace transformation of a function $f(t)$ is defined in the s domain by the following operation:

$$\bar{f}(s) \equiv L\{f(t)\} = \int_0^\infty f(t)e^{-st}dt. \tag{5}$$

Its application to the concentration quantities gives

$$\begin{aligned} L\{\gamma_i\} &= \bar{\gamma}_i \\ L\left\{\frac{\partial \gamma_i}{\partial t}\right\} &= s\bar{\gamma}_i - \gamma_i^0, \end{aligned} \tag{6}$$

so that **(1)** becomes

$$\begin{aligned} s\bar{\gamma}_1 - \bar{\gamma}_1^0 &= D_{11}\frac{\partial^2 \bar{\gamma}_1}{\partial r^2} + D_{12}\frac{\partial^2 \bar{\gamma}_2}{\partial r^2} \\ s\bar{\gamma}_2 - \bar{\gamma}_2^0 &= D_{21}\frac{\partial^2 \bar{\gamma}_1}{\partial r^2} + D_{22}\frac{\partial^2 \bar{\gamma}_2}{\partial r^2}. \end{aligned} \tag{7}$$

GENERAL SOLUTIONS

Define the quantities μ_i from the following equations:

$$\begin{aligned} \bar{\gamma}_1 &= H\mu_1 - F\mu_2 \\ \bar{\gamma}_2 &= -G\mu_1 + E\mu_2, \end{aligned} \tag{8}$$

where E, F, G, and H (following Fujita and Gosting symbolism[6]) are

$$E = \frac{D_{11}}{|D|}, \quad F = \frac{D_{12}}{|D|}, \quad G = \frac{D_{21}}{|D|}, \quad H = \frac{D_{22}}{|D|}, \tag{9}$$

with the determinant

$$|D| = \begin{vmatrix} D_{11} & D_{12} \\ D_{21} & D_{22} \end{vmatrix}.$$

Differentiating **(8)** with respect to r, we obtain

$$\begin{aligned} \frac{\partial^2 \mu_1}{\partial r^2} &= D_{11}\frac{\partial^2 \bar{\gamma}_1}{\partial r^2} + D_{12}\frac{\partial^2 \bar{\gamma}_2}{\partial r^2} \\ \frac{\partial^2 \mu_2}{\partial r^2} &= D_{21}\frac{\partial^2 \bar{\gamma}_1}{\partial r^2} + D_{22}\frac{\partial^2 \bar{\gamma}_2}{\partial r^2}. \end{aligned} \tag{10}$$

Inserting **(8)** and **(10)** into **(7)**, we obtain

$$\begin{aligned} \frac{\partial^2 \mu_1}{\partial r^2} &= -\gamma_1^0 + s\bar{\gamma}_1 = -\gamma_1^0 + s(H\mu_1 - F\mu_2) \\ \frac{\partial^2 \mu_2}{\partial r^2} &= -\gamma_2^0 + s\bar{\gamma}_2 = -\gamma_2^0 + s(E\mu_2 - G\mu_1). \end{aligned} \tag{11}$$

Differentiating **(11)** with respect to r twice, we obtain

$$\begin{aligned} \frac{\partial^4 \mu_1}{\partial r^4} &= s\left(H\frac{\partial^2 \mu_1}{\partial r^2} - F\frac{\partial^2 \mu_2}{\partial r^2}\right) \\ \frac{\partial^4 \mu_2}{\partial r^4} &= s\left(E\frac{\partial^2 \mu_2}{\partial r^2} - G\frac{\partial^2 \mu_1}{\partial r^2}\right). \end{aligned} \tag{12}$$

It now remains to uncouple the two differential equations **(12)** so that μ_1 and μ_2 do not depend on each other. From Equations **(11)** we can write:

$$\begin{aligned} \frac{\partial^2 \mu_1}{\partial r^2} &= -\gamma_1^0 - sF\mu_2 + \frac{H}{G}\left(-\gamma_2^0 + sE\mu_2 - \frac{\partial^2 \mu_2}{\partial r^2}\right) \\ \frac{\partial^2 \mu_2}{\partial r^2} &= -\gamma_2^0 - sG\mu_1 + \frac{E}{F}\left(-\gamma_1^0 + sH\mu_1 - \frac{\partial^2 \mu_1}{\partial r^2}\right), \end{aligned} \tag{13}$$

and inserting **(13)** into **(12)**, we have

$$\begin{aligned} \frac{\partial^2 \mu_1}{\partial r^4} - s(H+E)\frac{\partial^2 \mu_1}{\partial r^2} + s^2(EH - FG)\mu_1 &= s(E\gamma_1^0 + F\gamma_2^0) \\ \frac{\partial^2 \mu_2}{\partial r^4} - s(H+E)\frac{\partial^2 \mu_2}{\partial r^2} + s^2(EH - FG)\mu_2 &= s(G\gamma_1^0 + H\gamma_2^0). \end{aligned} \tag{14}$$

These are two uncoupled non-homogeneous differential equations. The characteristic equation related to the corresponding homogeneous differential equation, is

$$\lambda^4 - s(H+E)\lambda^2 + s^2(EH - FG) = 0, \tag{15}$$

from which we obtain two real negative physical solutions

$$\begin{aligned} \lambda_1 &= -\left\{\frac{s}{2}[H+E+\sqrt{(E+H)^2+4FG}]\right\}^{1/2} = -\sqrt{\sigma_1}\sqrt{s} \\ \lambda_2 &= -\left\{\frac{s}{2}[H+E+\sqrt{(E+H)^2+4FG}]\right\}^{1/2} = -\sqrt{\sigma_2}\sqrt{s}. \end{aligned} \tag{16}$$

From **(14)** the form of the particular integrals is

$$\mu_i' = [\text{constant}]r. \tag{17}$$

Thus, imposing

$$\frac{\partial^4}{\partial r^4}\mu_i' = \frac{\partial^2}{\partial r^2}\mu_i' = 0$$

from **(17)**, we obtain

$$\begin{aligned} \mu_1' &= \frac{1}{s}\frac{E\gamma_1^0 + F\gamma_2^0}{EH - FG} \\ \mu_2' &= \frac{1}{s}\frac{G\gamma_1^0 + H\gamma_2^0}{EH - FG}. \end{aligned} \tag{18}$$

Defining

$$\alpha_i(r) = e^{-\sqrt{s\sigma_i}r}, \tag{19}$$

the solutions have the following form:

$$\begin{aligned} \mu_1 &= \theta_{11}\alpha_1(r) + \theta_{12}\alpha_2(r) + \frac{1}{s}\frac{E\gamma_1^0 + F\gamma_2^0}{EH - FG} \\ \mu_2 &= \theta_{21}\alpha_1(r) + \theta_{22}\alpha_2(r) + \frac{1}{s}\frac{G\gamma_1^0 + H\gamma_2^0}{EH - FG}, \end{aligned} \tag{20}$$

where the θ_{ij} values are determined by the boundary conditions. Differentiating **(20)** with respect to r twice,

$$\begin{aligned} \frac{\partial^2 \mu_1}{\partial r^2} &= s[\theta_{11}\sigma_1\alpha_1(r) + \theta_{12}\sigma_2\alpha_2(r)] \\ \frac{\partial^2 \mu_2}{\partial r^2} &= s[\theta_{21}\sigma_1\alpha_1(r) + \theta_{22}\sigma_2\alpha_2(r)]. \end{aligned} \tag{21}$$

Substituting **(21)** into **(11)**,

$$\begin{aligned}
&\theta_{11} s\sigma_1 \alpha_1(r) + \theta_{12} s\sigma_2 \alpha_2(r) \\
&\quad = -\gamma_1^0 + sH[\theta_{11}\alpha_1(r) + \theta_{12}\alpha_2(r) + \mu_1'] - sG[\theta_{21}\alpha_1(r) + \theta_{22}\alpha_2(r) + \mu_2'] \\
&\theta_{21} s\sigma_1 \alpha_1(r) + \theta_{22} s\sigma_2 \alpha_2(r) \\
&\quad = -\gamma_2^0 + sE[\theta_{21}\alpha_1(r) + \theta_{22}\alpha_2(r) + \mu_2'] - sG[\theta_{11}\alpha_1(r) + \theta_{12}\alpha_2(r) + \mu_1'].
\end{aligned} \tag{22}$$

The identity between corresponding coefficients produces

$$\begin{aligned}
\theta_{21} &= \frac{H - \sigma_1}{F}\theta_{11} = \frac{G}{E - \sigma_1}\theta_{11} \\
\theta_{12} &= \frac{F}{H - \sigma_2}\theta_{22} = \frac{E - \sigma_2}{G}\theta_{22}.
\end{aligned} \tag{23}$$

The reduction to two coefficients, allows us to set

$$\begin{aligned}
K_1 &= \theta_{11}, \\
K_2 &= \theta_{22},
\end{aligned} \tag{24}$$

so that **(20)** becomes

$$\begin{aligned}
\mu_1 &= K_1\alpha_1(r) + \frac{F}{H - \sigma_2}K_2\alpha_2(r) + \mu_1' \\
\mu_2 &= \frac{G}{E - \sigma_1}K_1\alpha_1(r) + K_2\alpha_2(r) + \mu_2',
\end{aligned} \tag{25}$$

and from **(8)**, we obtain:

$$\begin{aligned}
\bar{\gamma}_1 &= \sigma_1 K_1\alpha_1(r) + \frac{F\sigma_2}{H - \sigma_2}K_2\alpha_2(r) + \frac{\bar{\gamma}_1^0}{s} \\
\bar{\gamma}_2 &= \frac{G\sigma_1}{E - \sigma_1}K_1\alpha_1(r) + \sigma_2 K_2\alpha_2(r) + \frac{\bar{\gamma}_2^0}{s}.
\end{aligned} \tag{26}$$

BOUNDARY CONDITIONS

Further specialization of integral solutions **(26)** needs the determination of K_i values, which are obtained by specifying the boundary conditions. Since we have assumed the cell is large with respect to the crystal dimensions, the restrictions imposed by the cell wall are not considered (free diffusion). The only boundary conditions that need to be considered are related to the crystal-solution interface.

The crystal growth rate, da/dt, where a is the crystal radius, is in general a complicated function of the supersaturation $\sigma = (c_1^i - c_1^e)/c_1^e$ at the crystal interface, where c_1^i is the concentration of the protein at the interface and c_1^e is the concentration in equilibrium with the crystal for a given concentration c_2^i of the precipitant. However, in several cases, the growth rate can be reasonably and conveniently expressed by the following linear function of the supersaturation:[2]

$$\frac{da}{dt} = \beta(\sigma - \sigma_0), \tag{27}$$

where β is a kinetic constant and σ_0 indicates the minimum supersaturation required for the crystal to grow.

The solutes fluxes, J_1^i and J_2^i, at the interface $r = a$, are defined by

$$\begin{aligned} -J_1^i &= D_{11}\frac{\partial c_1}{\partial r}\bigg|_{r=a} + D_{12}\frac{\partial c_2}{\partial r}\bigg|_{r=a} \\ -J_2^i &= D_{21}\frac{\partial c_1}{\partial r}\bigg|_{r=a} + D_{22}\frac{\partial c_2}{\partial r}\bigg|_{r=a}. \end{aligned} \tag{28}$$

The mass balance at the interface is described by the following equations:[2]

$$\begin{aligned} -J_1^i &= \left(c_1^s - c_1^i\frac{\rho_s}{\rho_l}\right)\frac{da}{dt} \\ -J_2^i &= \left(c_2^s - c_2^i\frac{\rho_s}{\rho_l}\right)\frac{da}{dt}, \end{aligned} \tag{29}$$

where c_i^s denotes the concentration of solute i in the solid phase, ρ_s is the solid phase density, and ρ_l is the liquid phase density. Balance equations **(29)** regard the net fluxes as the difference between the rate of solute insertion into the crystal and the rate of solutes rejection due to the replacement of the fluid solution with the new crystalline phase. Note that since the crystal is growing in the positive r direction, the protein flux towards the crystal is negative whereas its interface gradient is positive.

Rigorously speaking, the growing crystal gives rise to a moving boundary problem that will cause changes in a. If the crystal geometry were rectangular, both setting the frame at the crystal interface and using the free diffusion condition would not give rise to any loss of rigor in the treatment. However, the spherical geometry associated with the growing crystal imposes a curvature change that should be taken into account. If the radius is large and the curvature changes are small relative to the crystal growth rate, then the approximation of letting a be constant becomes reasonable.[2]

The analytic expressions for the inverse Laplace transformation are available[7] if the boundary equations can be expressed in the following way:

$$\begin{aligned} D_{11}\frac{\partial c_1}{\partial r}\bigg|_{r=a} + D_{12}\frac{\partial c_2}{\partial r}\bigg|_{r=a} &= h_1(c_1^i - c_1^*) \\ D_{21}\frac{\partial c_1}{\partial r}\bigg|_{r=a} + D_{22}\frac{\partial c_2}{\partial r}\bigg|_{r=a} &= h_2(c_1^i - c_1^*), \end{aligned} \tag{30}$$

where the h_i and the c_1^* are constants. The expression for these parameters can be obtaining inserting **(27)** and **(29)** into **(28)**,

$$\begin{aligned} -J_1^i &= \left(c_1^s - c_1^i\frac{\rho_s}{\rho_l}\right)\frac{\beta}{c_1^e}[c_1^i - c_1^e(1+\sigma_0)] = h_1(c_1^i - c_1^*) \\ -J_2^i &= \left(c_2^s - c_2^i\frac{\rho_s}{\rho_l}\right)\frac{\beta}{c_1^e}[c_1^i - c_1^e(1+\sigma_0)] = h_2(c_1^i - c_1^*), \end{aligned} \tag{31}$$

where

$$
\begin{aligned}
c_1^* &= c_1^e(1+\sigma_0) \\
h_1 &= \left(c_1^s - c_1^i\frac{\rho_s}{\rho_l}\right)\frac{\beta}{c_1^e} \\
h_2 &= \left(c_2^s - c_2^i\frac{\rho_s}{\rho_l}\right)\frac{\beta}{c_1^e}.
\end{aligned}
\tag{32}
$$

We can see that c_1^* is constant if and only if c_1^e is constant. From solubility theory we expect that the protein equilibrium concentration is given approximately by the following equation:[8,9]

$$c_1^e = ce^{-kc_2^i}, \tag{33}$$

where c and k are constants. Since we expect that c_2^i is not so different from c_2^0, we can reasonably assume that $c_1^e \approx c_1^{e0} \equiv ce^{-kc_2^s}$ is roughly constant. We can then write

$$c_1^* \approx c_1^{e0}(1+\sigma_0). \tag{34}$$

The concentration c_1^i is small with respect to c_1^s, whereas the crystal density is only slightly larger than the solution density, thus[2] $c_1^s >> c_1^i\,\rho_s/\rho_l$. We can now reasonably assume that h_1 is constant and equal to

$$h_1 \approx \beta\frac{c_1^*}{c_1^{e0}}. \tag{35}$$

The concentration of salt in the solid can be estimated by the repartition constant, α, defined by the following equation:[10]

$$\alpha = \frac{c_2^s/c_1^s}{c_2^i/c_1^i} \cong \frac{c_2^s/c_1^s}{c_2^0/c_1^0}. \tag{36}$$

It is reasonable to assume that h_2 is constant and given by

$$h_2 \approx \beta\frac{c_2^0}{c_1^{e0}}\left(\alpha\frac{c_1^s}{c_1^0} - \frac{\rho_s}{\rho_l}\right). \tag{37}$$

Note that h_1 is always positive because it describes the protein mass transfer. On the other hand, h_2 is negative because the precipitant rejection caused by the crystal growth is larger than the contribution due to the salt inclusion into the crystal. Hence, the protein flux is negative, whereas the precipitant flux is positive.

CONCENTRATION PROFILES

From the definition of γ_i, we can write

$$\frac{\partial c_i}{\partial r} = \frac{\partial}{\partial r}(\gamma_i/r) = \frac{1}{r}\frac{\partial\gamma_i}{\partial r} - \frac{1}{r^2}\gamma_i, \tag{38}$$

and by defining $\bar{\gamma}_i^* \equiv c_1^* a/s$, **(30)** becomes:

$$
\begin{aligned}
D_{11}\left(\frac{\partial\bar{\gamma}_1}{\partial r}\bigg|_{r=a} - \frac{\bar{\gamma}_1^i}{a}\right) + D_{12}\left(\frac{\partial\bar{\gamma}_2}{\partial r}\bigg|_{r=a} - \frac{\bar{\gamma}_2^i}{a}\right) &= h_1(\bar{\gamma}_1^i - \bar{\gamma}_1^*)\\
D_{21}\left(\frac{\partial\bar{\gamma}_1}{\partial r}\bigg|_{r=a} - \frac{\bar{\gamma}_1^i}{a}\right) + D_{22}\left(\frac{\partial\bar{\gamma}_2}{\partial r}\bigg|_{r=a} - \frac{\bar{\gamma}_2^i}{a}\right) &= h_2(\bar{\gamma}_1^i - \bar{\gamma}_1^*).
\end{aligned}
\tag{39}
$$

To obtain the K_i, we need to insert the general solutions into **(39)**. First note that from **(39)**,

$$
\begin{aligned}
-\frac{\partial\bar{\gamma}_1}{\partial r}\bigg|_{r=a} &= \sqrt{s}\left[\sigma_1^{3/2}K_1\alpha_1(r) + \frac{F\sigma_2^{3/2}}{H-\sigma_2}K_2\alpha_2(r) + \frac{c_1^0}{s}\right]\\
-\frac{\partial\bar{\gamma}_2}{\partial r}\bigg|_{r=a} &= \sqrt{s}\left[\frac{G\sigma_1^{3/2}}{E-\sigma_1}K_1\alpha_1(r) + \sigma_2^{3/2}K_2\alpha_2(r) + \frac{c_2^0}{s}\right]
\end{aligned}
\tag{40}
$$

and

$$
\begin{aligned}
-\left(\frac{\partial\bar{\gamma}_1}{\partial r}\bigg|_{r=a} - \frac{\bar{\gamma}_1^i}{a}\right) &= \sigma_1^{3/2}K_1\alpha_1(r)\left(\frac{1}{a} + \sqrt{s}\sqrt{\sigma_1}\right) + \frac{F\sigma_2^{3/2}}{H-\sigma_2}K_2\alpha_2(r)\left(\frac{1}{a} + \sqrt{s}\sqrt{\sigma_2}\right)\\
-\left(\frac{\partial\bar{\gamma}_2}{\partial r}\bigg|_{r=a} - \frac{\bar{\gamma}_2^i}{a}\right) &= \frac{G\sigma_1^{3/2}}{E-\sigma_1}K_1\alpha_1(r)\left(\frac{1}{a} + \sqrt{s}\sqrt{\sigma_1}\right) + \sigma_2^{3/2}K_2\alpha_2(r)\left(\frac{1}{a} + \sqrt{s}\sqrt{\sigma_2}\right),
\end{aligned}
\tag{41}
$$

then, inserting **(41)** into **(39)**

$$
\begin{aligned}
(P_{11} + \sqrt{s}Q_{11})\alpha_1(r)K_1 + (P_{12} + \sqrt{s}Q_{12})\alpha_2(r)K_2 &= \frac{B_1}{s}\\
(P_{21} + \sqrt{s}Q_{21})\alpha_1(r)K_1 + (P_{22} + \sqrt{s}Q_{22})\alpha_2(r)K_2 &= \frac{B_2}{s},
\end{aligned}
\tag{42}
$$

where

$$
\begin{aligned}
P_{11} &= \left(D_{11}\sigma_1 + D_{12}\frac{G\sigma_1}{E-\sigma_1}\right)\frac{1}{a} + h_1\sigma_1\\
P_{12} &= \left(D_{11}\frac{F\sigma_2}{H-\sigma_2} + D_{12}\sigma_2\right)\frac{1}{a} + h_1\frac{F\sigma_2}{H-\sigma_2}\\
P_{21} &= \left(D_{21}\sigma_1 + D_{22}\frac{G\sigma_1}{E-\sigma_1}\right)\frac{1}{a} + h_2\sigma_1\\
P_{22} &= \left(D_{21}\frac{F\sigma_2}{H-\sigma_2} + D_{22}\sigma_2\right)\frac{1}{a} + h_2\frac{F\sigma_2}{H-\sigma_2}
\end{aligned}
\tag{43}
$$

$$
\begin{aligned}
Q_{11} &= \left(D_{11}\sigma_1 + D_{12}\frac{G\sigma_1}{E-\sigma_1}\right)\sqrt{\sigma_1}\\
Q_{12} &= \left(D_{11}\frac{F\sigma_2}{H-\sigma_2} + D_{12}\sigma_2\right)\sqrt{\sigma_2}\\
Q_{21} &= \left(D_{21}\sigma_1 + D_{22}\frac{G\sigma_1}{E-\sigma_1}\right)\sqrt{\sigma_1}\\
Q_{22} &= \left(D_{21}\frac{F\sigma_2}{H-\sigma_2} + D_{22}\sigma_2\right)\sqrt{\sigma_2}
\end{aligned}
\tag{44}
$$

$$\begin{aligned} B_1 &= -h_1 a(c_1^0 - c_1^*) \\ B_2 &= -h_2 a(c_1^0 - c_1^*). \end{aligned} \tag{45}$$

By setting

$$\begin{aligned} R_1 &= B_1 P_{22} - B_2 P_{12} \\ R_2 &= B_2 P_{11} - B_1 P_{21} \\ S_1 &= B_1 Q_{22} - B_2 Q_{12} \\ S_2 &= B_2 Q_{11} - B_1 Q_{21} \\ T &= P_{11} P_{22} - P_{12} P_{21} \\ U &= Q_{11} P_{22} + P_{11} Q_{22} - Q_{12} P_{21} - P_{12} Q_{21} \\ V &= Q_{11} Q_{22} - Q_{12} Q_{21} \end{aligned} \tag{46}$$

we obtain

$$\begin{aligned} K_1 &= \frac{1}{s}\alpha_1(-a)\frac{R_1 + S_1\sqrt{s}}{T + U\sqrt{s} + Vs} = \frac{1}{s}\alpha_1(-a)\left(\frac{M_{11}}{\sqrt{s} - s_1} + \frac{M_{12}}{\sqrt{s} - s_2}\right) \\ K_2 &= \frac{1}{s}\alpha_2(-a)\frac{R_2 + S_2\sqrt{s}}{T + U\sqrt{s} + Vs} = \frac{1}{s}\alpha_2(-a)\left(\frac{M_{12}}{\sqrt{s} - s_1} + \frac{M_{22}}{\sqrt{s} - s_2}\right), \end{aligned} \tag{47}$$

where

$$\begin{aligned} s_1 &= \frac{1}{2}\left[+\sqrt{\left(\frac{U}{V}\right)^2 - 4\frac{T}{V}}\right] \\ s_2 &= \frac{1}{2}\left[-\sqrt{\left(\frac{U}{V}\right)^2 - 4\frac{T}{V}}\right] \end{aligned} \tag{48}$$

$$\begin{aligned} M_{11} &= \frac{S_1 s_1 + R_1/S_1}{V}\frac{}{s_1 - s_2} \\ M_{12} &= -\frac{S_1 s_2 + R_1/S_1}{V}\frac{}{s_1 - s_2} \\ M_{21} &= \frac{S_2 s_1 + R_2/S_2}{V}\frac{}{s_1 - s_2} \\ M_{22} &= -\frac{S_2 s_2 + R_2/S_2}{V}\frac{}{s_1 - s_2}. \end{aligned} \tag{49}$$

This defines the K_i as functions of s. We can now apply the inverse Laplace transformation $L^{-1}\{\cdot\}$ to $\bar{\gamma}_i$. Since,[7]

$$L^{-1}\left\{\frac{1}{s}\frac{\alpha_i(r-a)}{\sqrt{s} - s_j}\right\} = -\frac{1}{\sqrt{s_j}}\chi_{ij}(r-a;t), \tag{50}$$

where

$$\chi_{ij}(r-a;t) = \operatorname{erfc}\left[\frac{\sqrt{\sigma_i}(r-a)}{2\sqrt{t}}\right] - e^{-s_j\sqrt{\sigma_i}(r-a)+s_j t}\operatorname{erfc}\left[\frac{\sqrt{\sigma_i}(r-a)}{2\sqrt{t}} - s_j t\right] \quad \textbf{(51)}$$

and $\operatorname{erfc}(z) = 1 - \operatorname{erf}(z)$. We finally obtain the analytic expressions for the concentration profiles

$$\begin{aligned} c_1 &= c_1^0 + \frac{1}{r}\left[\sigma_1\Phi_1(r-a;t) + \frac{F\sigma_2}{H-\sigma_2}\Phi_2(r-a;t)\right] \\ c_2 &= c_2^0 + \frac{1}{r}\left[\frac{G\sigma_1}{E-\sigma_1}\Phi_1(r-a;t) + \sigma_2\Phi_2(r-a;t)\right], \end{aligned} \quad \textbf{(52)}$$

where:

$$\begin{aligned} \Phi_1(r-a;t) &= \frac{M_{11}}{s_1}\chi_{11}(r-a;t) + \frac{M_{12}}{s_2}\chi_{12}(r-a;t) \\ \Phi_2(r-a;t) &= \frac{M_{21}}{s_1}\chi_{21}(r-a;t) + \frac{M_{22}}{s_2}\chi_{22}(r-a;t). \end{aligned} \quad \textbf{(53)}$$

RESULTS

For a typical lysozyme crystal growth process in aqueous sodium chloride, we consider the following experimental conditions and system physicochemical properties:[11–15]

$c_1^0 = 0.0035\,\text{mol}\cdot\text{dm}^{-3}$	$a = 0.1\,\text{cm}$	$D_{11} = 0.1\times10^{-5}\,\text{cm}^2\,\text{sec}^{-1}$
$c_2^0 = 0.5\,\text{mol}\cdot\text{dm}^{-3}$	$\beta = 1\times10^{-7}$ cm/sec	$D_{12} = 0.0001\times10^{-5}\,\text{cm}^2\,\text{sec}^{-1}$
$\sigma = 15$	$\sigma_0 = 3$	$D_{21} = 15\times10^{-5}\,\text{cm}^2\,\text{sec}^{-1}$
	$\alpha = 0.01$	$D_{22} = 1.5\times10^{-5}\,\text{cm}^2\,\text{sec}^{-1}$
$c_1^s = 0.06\,\text{mol}\cdot\text{dm}^{-3}$		
$\rho_s = 1.2\,\text{g}\cdot\text{cm}^{-3}$		
$\rho_l = 1.0\,\text{g}\cdot\text{cm}^{-3}$		

FIGURE 1 gives the *protein* concentration profiles around the crystal for a given set of time values (1′, 10′, 30′, 2 h, 6 h, 1 day, and 5 days). The presence of a depletion zone around the crystal is visible, and its width is expanding with time. However, the absence of large salt gradients and the consequent small contribution in the protein flux gives rise to marginal coupling effects, so that the protein concentration profiles are well approximated by the uncoupled transport process. Thus, the coefficient D_{12} is not a relevant parameter for the crystal growth scenario; however, this conclusion does not preclude the importance of the coefficient during the nucleation stage not contained in the model.

FIGURE 2 gives the *precipitant* concentration profiles around the crystal for the same set of times and for both a coupled and an uncoupled scenario. The salt concentration profiles seem to be significantly affected by the interaction of the fluxes, and at the interfacial concentration, the results seem to be larger for the coupled case.

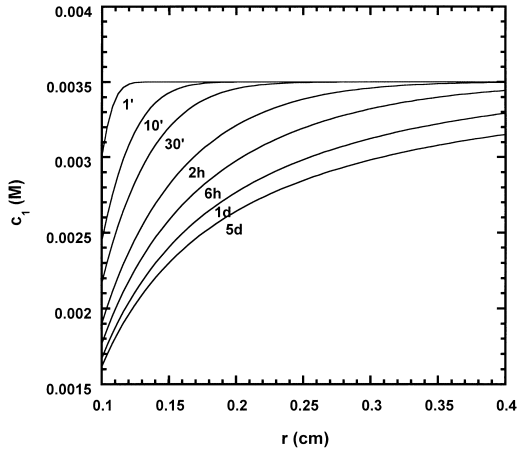

FIGURE 1. Protein concentration profiles around the crystal for time values 1′, 10′, 30′, 2 h, 6 h, 1 day, and 5 days.

A parameter that may quantify the effect of the coupled transport on the precipitant interfacial concentration is the stationary salt concentration excess defined by

$$\chi = \lim_{t \to \infty} \left(\frac{c_2^i}{c_2^0} \right). \tag{54}$$

From FIGURE 2, we see that slight precipitant concentration excesses are present for the uncoupled case, which are also being caused by the crystal growth wall effect. A

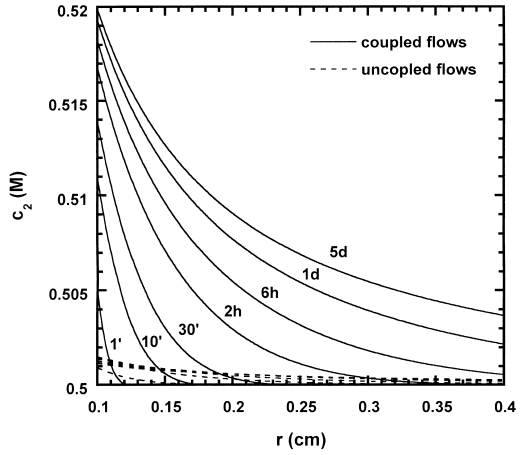

FIGURE 2. Precipitant concentration profiles around the crystal for time values 1′, 10′, 30′, 2 h, 6 h, 1 day, and 5 days. The *solid lines* refer to the coupled scenario; the *dashed lines* refer to the uncoupled scenario.

numerical analysis was performed to examine how the relevant system variables may influence χ. The results were as follows:

1. changing D_{21}/D_{11} from 0 to 400 changes χ from 1.004 to 1.128;
2. changing D_{21}/D_{22} from 10 to 30 changes χ from 1.052 to 1.152; and
3. changing σ from 5 to 100 changes χ from 1.030 to 1.072.

Another important variable for the overall crystallization process is the kinetic Peclet number[16] defined by $Pe_k = \beta\delta/D_{11}$, where δ is the width of the diffusion layer and can be estimated from

$$\delta \approx \frac{c_1^0 - c_1^i}{\left.\dfrac{\partial c_1}{\partial r}\right|_{r=a}}.$$

In our case, the diffusion layer width was found to be roughly 0.1cm. The kinetic Peclet number is the controlling parameter that gives the relative importance of the transport mechanism with respect to the incorporation kinetics. For instance, values of $Pe_k << 0.1$ or $Pe_k >> 0.1$ indicate, respectively, purely kinetic or transport controlled growth. A numerical analysis shows that changing the kinetic Peclet number from 0.1 to 10, χ changes from 1.014 to 1.070.

Lin *et al.*[2] reported an incorrect interpretation of the coupling transport between salt and protein. The coupled transport was attributed to the association between the macromolecules and the ions giving rise to the depletion of the salt concentration at the crystal interface. In contrast, this simulation yields an interfacial salt enrichment that is caused by electrostatic coupling between both ions and excluded volume effects. Since the partition constant α defined by **(36)** was used to describe the precipitant concentration inside the crystal, the model cannot predict non-uniform precipitant distribution within the solid phase. However, due to the time dependence of the interfacial precipitant concentration (and of the precipitant chemical potential), non-uniform precipitant incorporation can be presumed. This may cause strain in the crystal and ultimately compromise crystal size and quality.

CONCLUSIONS

For the system lysozyme chloride + NaCl + H_2O at relatively low protein concentrations the effect of the inclusion of cross-term diffusion coefficients does effect the calculation of precipitant concentration distribution about the growing crystal and should be included when modeling crystal growth. This will be possible if general schemes for estimating the diffusion coefficients in multicomponent systems containing a protein become available. However for the model calculations considered here the effect causes only small changes of crystal face precipitant concentrations, but this effect could nevertheless be important. Finally, it should be noted that the diffusion coefficients depend on concentration and that if the diffusion coefficient changes are sufficiently large within a system, then numerical analysis methods are necessary.

ACKNOWLEDGMENTS

J.G.A. notes that this paper is taken directly from chapter 19 of the Ph.D. dissertation[17] (ISBN 0-493-12797-6) of the first author who deserves full credit for this work. The support of the NASA Microgravity Biotechnology Program through Grant NAG8-1356 is gratefully acknowledged. Support from Texas Christian University Grant RCAF-11950 is also gratefully acknowledged.

REFERENCES

1. ROSENBERGER, F. 1986. Inorganic and protein crystal growth—similarities and differences. J. Cryst. Growth **76:** 618–636.
2. LIN, H., *et al.* 1995. Convective-diffusive transport in protein crystal growth. J. Cryst. Growth **151:** 153–162.
3. MCPHERSON, A., *et al.* 1999 The effects of microgravity on protein crystallization: evidence for concentration gradients around growing crystals. J. Cryst. Growth **196:** 572–586.
4. MCPHERSON, A. 1999. Crystallization of Biological Macromolecules. CSHL Press, New York.
5. CRANK, J. 1975. The Mathematics of Diffusion. Clarendon Press, Oxford.
6. FUJITA, H. & L.J. GOSTING. 1960. A new procedure for calculating the four diffusion coefficients of three-component systems from Gouy diffusiometer data. J. Phys. Chem. **64:** 1256–1263.
7. CHURCHILL, R.V. 1958. Operational Mathematics. McGraw-Hill, New York.
8. ARAKAWA, T. & S.N. TIMASHEFF. 1985. Theory of protein solubility. *In* Methods in Enzymology, Vol. 114. H.W. Wyckoff, C.H.W. Hirs & S.N. Timasheff, Eds.: 49–77. Academic Press, New York.
9. GREEN, A.A. 1932. Studies in the physical chemistry of proteins. X. The solubility of hemoglobin in solutions of chlorides and sulfates of varying concentrations. J. Biol. Chem. **95:** 47–66.
10. VEKILOV, P.G., *et al.* 1996. Repartitioning of NaCl and protein impurities in lysozyme crystallization. Acta Crystallogr. Sect. D **52:** 785–798.
11. ALBRIGHT, J.G., *et al.* 1999. Precision measurements of binary and multicomponent diffusion coefficients in protein soutions relevant to crystal growth: lysozyme chloride in water and aqueous NaCl at pH 4.5 and 25°C. J. Am. Chem. Soc. **121:** 3256–3266.
12. ANNUNZIATA, O., *et al.* 2000. Extraction of thermodynamic data from ternary diffusion coefficients. Use of precision diffusion measurements for aqueous lysozyme chloride-NaCl at 25°C to determine the charge of lysozyme chloride chemical potential with increasing NaCl concentration well into the supersaturated region. J. Am. Chem. Soc. **122:** 5916–5928.
13. GOSTING, L.J. 1956. Measurement and interpretation of diffusion coefficients of proteins. *In* Advances in Protein Chemistry, Vol. 11. M.L. Anson, K. Bailey & J.T. Edsall, Eds.: 429–555. Academic Press, New York.
14. STEINRAUF, L.K. 1959. Preliminary X-ray data for some new crystalline forms of β-lactoglobulin and hen egg-white lysozyme. Acta Cryst. **12:** 77–78.
15. MONACO, L.A. & F. ROSENBERGER. 1993. Growth and etching kinetics of tetragonal lysozyme. J. Cryst. Growth **129:** 465–484.
16. VEKILOV, P.G., *et al.* 1996. Nonlinear response of layer growth dynamics in mixed kinetics-bulk transport regime. Phys. Rev. E **54:** 6650–6660.
17. ANNUNZIATA, O. 2001. Analysis of the Protein-Salt Coupled Transport. Ph.D. Dissertation, Texas Christian University, Fort Worth.